Empirical Hα emitter count predictions for dark energy surveys

J. E. Geach,[1]⋆ A. Cimatti,[2] W. Percival,[3] Y. Wang,[4] L. Guzzo,[5] G. Zamorani,[6]
P. Rosati,[7] L. Pozzetti,[6] A. Orsi,[1] C. M. Baugh,[1] C. G. Lacey,[1] B. Garilli,[8]
P. Franzetti,[8] J. R. Walsh[7] and M. Kümmel[7]

[1]*Institute for Computational Cosmology, Department of Physics, Durham University, South Road, Durham DH1 3LE*
[2]*Dipartimento di Astronomica, Universita di Bologna, via Ranzani 1, I-40127 Bologna, Italy*
[3]*Institute of Cosmology and Gravitation, University of Portsmouth, Dennis Sciama building, Portsmouth PO1 3FX*
[4]*Homer L. Dodge Department of Physics & Astronomy, The University of Oklahoma, 440 W. Brooks St., Norman, OK 73019, USA*
[5]*INAF, Osservatorio Astronomico di Brera, via Bianchi 46, I-23807 Merate (LC), Italy*
[6]*INAF, Osservatorio Astronomico di Bologna, via Ranzani 1, 40127 Bologna, Italy*
[7]*Space Telescope European Co-Ordinating Facility, European Southern Observatory, Karl Schwarzschild Str. 2, D-85748 Garching bei München, Germany*
[8]*INAF – IASF Milano, via E. Bassini 15, I-20133 Milan, Italy*

ABSTRACT

Future galaxy redshift surveys aim to measure cosmological quantities from the galaxy power spectrum. A prime example is the detection of baryonic acoustic oscillations, providing a standard ruler to measure the dark energy equation of state, $w(z)$, to high precision. The strongest practical limitation for these experiments is how quickly accurate redshifts can be measured for sufficient galaxies to map the large-scale structure. A promising strategy is to target emission-line (i.e. star-forming) galaxies at high redshift ($z \sim 0.5$–2); not only is the space density of this population increasing out to $z \sim 2$, but also emission lines provide an efficient method of redshift determination. Motivated by the prospect of future dark energy surveys targeting Hα emitters at near-infrared wavelengths (i.e. $z > 0.5$), we use the latest empirical data to model the evolution of the Hα luminosity function out to $z \sim 2$ and thus provide predictions for the abundance of Hα emitters for practical limiting fluxes. We caution that the estimates presented in this work must be tempered by an efficiency factor, ϵ, giving the redshift success rate from these potential targets. For a range of practical efficiencies and limiting fluxes, we provide an estimate of $\bar{n} P_{0.2}$, where $\bar{n}$ is the 3D galaxy number density and $P_{0.2}$ is the galaxy power spectrum evaluated at $k = 0.2 \, h \, \text{Mpc}^{-1}$. Ideal surveys must provide $\bar{n} P_{0.2} > 1$ in order to balance shot-noise and cosmic variance errors. We show that a realistic emission-line survey ($\epsilon = 0.5$) could achieve $\bar{n} P_{0.2} = 1$ out to $z \sim 1.5$ with a limiting flux of $10^{-16} \, \text{erg s}^{-1} \, \text{cm}^{-2}$. If the limiting flux is a factor of 5 brighter, then this goal can only be achieved out to $z \sim 0.5$, highlighting the importance of survey depth and efficiency in cosmological redshift surveys.

Key words: galaxies: evolution – galaxies: high-redshift – cosmology: observations – large-scale structure of Universe.

1 INTRODUCTION

One of the greatest challenges the current generation of cosmologists faces is to understand the physics underlying the apparent acceleration of the expansion of the Universe (e.g. Riess et al. 1998; Perlmutter et al. 1999). Contemporary models favour the influence of a dark energy that has come to dominate the energy density of the universe during the last 8 billion years. Unfortunately, dark energy is

outside the realm of the standard model and requires new physics to explain. Nevertheless, many mechanisms have been proposed, and the potential for establishing which (if any) is correct experimentally has caused great fervour amongst the astronomical community over the past decade. The reward for investing a large amount of effort into determining the physics of dark energy is of course a profound advancement of our understanding of the fundamental nature of the universe.

A range of dark energy models exist (see Peebles & Ratra 2003; Copeland, Mizuno & Shaeri 2009 for reviews); however, the two most prominent scenarios attribute the accelerating expansion to

⋆E-mail: j.e.geach@durham.ac.uk

(i) a 'cosmological constant' (Λ) analogous to a non-zero quantum mechanical vacuum energy that has now come to dominate the overall energy density of the universe (but 120 orders of magnitude smaller than the value predicted by quantum physics) or (ii) a dynamic scalar field ('quintessence') which varies with both time and space. Both models require general relativity to hold on cosmological scales. A third alternative to explain the acceleration is the failure of general relativity on large scales, such that the gravity theory itself needs to be modified (e.g. Dvali, Gabadadze & Porrati 2000).

One way of distinguishing Λ from quintessence is to measure the evolution of the expansion of the universe, which is controlled by the dark energy equation of state, $w(z)$: the ratio of dark energy pressure P to density ρ. For Λ models, $\rho = -P/c^2$ for all time, such that $w(z) = -1$. Detecting a varying $w(z)$ would be a possible indication for quintessence. However, if gravity is modified, such behaviour could be just an indirect effect of the failure of general relativity. Such degeneracy between dark energy and modified gravity can be lifted only by measuring the growth rate of cosmic structure $f(z)$ [or its integral $G(z)$], which is governed by the interplay between the strength of gravity and the expansion rate of the Universe. Thus, measuring $w(z)$ and $f(z)$ as a function of redshift represents the most powerful combination of observational probes to distinguish among competing models (Guzzo et al. 2008; Wang 2008). This is the primary goal of current and future dark energy surveys (Albrecht et al. 2009).

Although the accelerated expansion was discovered using observations of Type Ia supernovae (Riess et al. 1998; Perlmutter et al. 1999), results from these observations are now dominated by systematic errors (e.g. Hicken et al. 2009). Future studies of dark energy therefore aim to exploit different observations and of those proposed, the use of baryon acoustic oscillations (BAO) as standard rulers appears to have the lowest level of systematic uncertainty (Albrecht et al. 2006). BAO are a series of peaks and troughs in the power spectrum, which quantifies the clustering strength of matter as a function of scale. They occur because primordial cosmological perturbations excite sound waves in the relativistic plasma of the early universe: when the plasma breaks down at recombination, the radiation can be observed as the cosmic microwave background (CMB), while the fluctuations in the baryonic material give rise to BAO (Silk 1968; Peebles & Yu 1970; Sunyaev & Zel'dovich 1970; Bond & Efstathiou 1984, 1987; Holtzman 1989). The BAO signal is on large scales, which are predominantly in the linear regime today. It is therefore expected that BAO should also be seen in the galaxy distribution (Goldberg & Strauss 1998; Meiksin, White & Peacock 1999; Seo & Eisenstein 2005; Springel et al. 2005; White 2005; Eisenstein, Seo & White 2007; Kazin et al. 2009) and can be used as a standard ruler, leading to measurements of the angular diameter distance $D_A(z)$ and the Hubble expansion rate $H(z)$, and therefore $w(z)$ (Blake & Glazebrook 2003; Hu & Haiman 2003; Seo & Eisenstein 2003; Wang 2006).

The acoustic signature has now been convincingly detected at low redshift (Percival et al. 2001; Cole et al. 2005; Eisenstein et al. 2005; Huetsi 2006) using the 2 degree Field (2dF) Galaxy Redshift Survey (2dFGRS; Colless et al. 2003) and the Sloan Digital Sky Survey (SDSS; York et al. 2000). Further analyses of the SDSS have led to competitive constraints on cosmological models (Percival et al. 2007; Gaztanaga, Cabre & Hui 2009; Percival et al. 2009). Ongoing spectroscopic surveys aiming to use BAO to analyse dark energy include the Baryon Oscillation Spectroscopic Survey (BOSS; Schlegel, White & Eisenstein 2009), the Hobby-Eberly Dark Energy Experiment (HETDEX; Hill et al. 2008) and

the WiggleZ survey (Glazebrook et al. 2007). Ongoing photometric surveys such as the Dark Energy Survey (DES)[1] and the Panoramic Survey Telescope & Rapid Response System (Pan-STARRS)[2] aim to find BAO using photometric redshifts.

The power spectrum (or the correlation function) of the galaxy distribution also contains key information on the growth rate of structure $f(z)$ (Kaiser 1987). This produces large-scale motions towards density maxima, which contribute a peculiar velocity component to the measured galaxy redshifts used to reconstruct cosmic structure in 3D. The net effect is to produce an anisotropy in the power spectrum that can be measured to extract an estimate of the growth rate $f(z)$ modulo the bias factor of the galaxies being observed. The importance of this well-known effect in the context of dark energy has become evident only in recent times, when redshift surveys of sufficient size at $z \sim 1$ have started to become available (Guzzo et al. 2008). Thus, a redshift survey of galaxies provides us with the ability to obtain an estimate of two key probes of cosmic acceleration, the expansion rate and the growth rate.

In order to reduce shot-noise and cosmic variance in 'precision' measurements of BAO and redshift distortions, the ultimate observational challenge is to accurately measure a large number (tens or hundreds of millions) of redshifts for galaxies spread over a significant interval of cosmic time, spanning the transition from matter domination to dark energy domination in the universe and covering the majority of the extragalactic ($|b| > 20°$) sky, $\sim 2 \times 10^4$ deg^2. Such a survey can be conducted using a dedicated survey telescope from a space platform, as proposed by the Joint Dark Energy Mission (JDEM)[3] and European Space Agency's Euclid and SPACE satellite mission concepts[4] (Cimatti et al. 2009). Some of the ongoing and planned future BAO surveys, such as WiggleZ, will target emission-line galaxies – i.e. generally star-forming galaxies with easily identifiable redshifts. The goal of this work is to make a prediction for the abundance of Hα emitting galaxies that these dark energy surveys can expect using the existing empirical evidence of past and recent Hα surveys out to $z \sim 2$.

In this work, we use empirical data to build a simple phenomenological model of the evolution of the Hα luminosity function (LF) since $z \sim 2$ and therefore predict the number counts of Hα emitters in redshift ranges pertinent to future dark energy surveys (the empirical model can also be used as a fiducial point for semi-analytic predictions for the abundance of star-forming galaxies; e.g. Baugh et al. 2005; Bower et al. 2006; Orsi et al. 2009). In Section 2 we describe the model, list the principal predictions and draw the reader's attention to some important caveats. In Section 3 we discuss the implications of the number count predictions on planned dark energy surveys, and in Section 4 we comment on the relevance of cosmological surveys in the near-infrared (near-IR) from a terrestrial base. For luminosity estimates, throughout we assume a fiducial cosmological model of $H_0 = 70 \, \mathrm{km \, s^{-1} \, Mpc^{-1}}$, $\Omega_m = 0.3$ and $\Omega_\Lambda = 0.7$.

2 A SIMPLE MODEL OF THE EVOLUTION OF THE Hα LUMINOSITY DENSITY

Fortuitously for dark energy surveys, the global volume-averaged star formation rate increases steeply out to $z \sim 2$ and flattens (or

---

[1] http://www.darkenergysurvey.org
[2] http://pan-starrs.ifa.hawaii.edu
[3] http://jdem.gsfc.nasa.gov
[4] http://sci.esa.int/euclid

Table 1. Parameters of the LFs used to derive the empirical model of Hα counts. All Schechter function parameters have been corrected to a common fiducial cosmology ($H_0 = 70 \, \mathrm{km \, s^{-1} \, Mpc^{-1}}$, $\Omega_m = 0.3$, $\Omega_\Lambda = 0.7$).

| Reference | z | Schechter function parameters | | | EW$_0$ (Å) | Type |
		$\log L^\star$ (erg s^{-1})	$\log \phi^\star$ (Mpc^{-3})	α		
Gallego et al. (1995)	<0.045	41.87	−2.78	−1.3	>10	UCM survey
Shioya et al. (2008)	0.24	41.94	−2.65	−1.35	>9	Narrow-band 0.815 μm
Yan et al. (1999)	1.3 ± 0.5	42.83	−2.82	−1.35	∼10–130	*HST*/NICMOS grism 1.5 μm
Geach et al. (2008)	2.23 ± 0.03	42.83	−2.84	−1.35	>12	Narrow-band 2.121 μm

perhaps gently declines) towards earlier epochs (e.g. Lilly et al. 1995; Hopkins 2004). This will work in favour of dark energy surveys, provided the shape of the LF is reasonably well understood. Locally, star-forming galaxies can be easily selected using the well-calibrated and 'robust' Hα emission line at $\lambda = 6563$ Å (e.g. Gallego et al. 1995; Ly et al. 2007; Shioya et al. 2008). This is a favourable line to target at high redshift because it is the least affected by extinction (compared to, say, [O II]). The shape of the Hα LF in the local Universe is well characterized, and over the past decade, near-IR surveys have tracked the evolution of the LF out to $z \sim 2$ (McCarthy et al. 1999; Yan et al. 1999; Hopkins, Connolly & Szalay 2000; Moorwood et al. 2000). Furthermore, the increasing feasibility of statistically significant wide-field Hα surveys at high redshift has vastly improved our picture of how the Hα LF has evolved over the past 8 Gyr (e.g. Geach et al. 2008; Shim et al. 2009; Sobral et al. 2009).

2.1 Empirical fit

Throughout this work, we assume that the conventional form of the LF holds at all epochs – the Schechter function:

$$\phi(L)\mathrm{d}L = \phi^\star (L/L^\star)^\alpha \exp(-L/L^*)\mathrm{d}(L/L^\star). \qquad (1)$$

In Table 1 we list the Schechter function parameters derived from four Hα surveys spanning $0 < z < 2$, chosen for their similarity in fitting (all find or fix the faint-end slope $\alpha = -1.35$) and equivalent width (EW) cuts, generally EW$_0 > 10$ Å. Note that there is very little evolution in the LF between $z \sim 2$ and $z = 1.3$ (Yan et al. 1999; Geach et al. 2008), although both of these surveys *assume* a fixed faint-end slope of -1.35 similar to that found in the local Universe (necessitated by the depths of these surveys). In comparison, by $z \sim 0$, the characteristic luminosity $L^\star$ has dropped by an order of magnitude (Gallego et al. 1995). The evolution of the space density normalization $\phi^\star$ is harder to model – the values listed in Table 1 imply little evolution (compared to $L^\star$) with $\langle \phi^\star \rangle = 1.7 \times 10^{-3} \, \mathrm{Mpc^{-3}}$. However, other surveys have derived a larger range of $\phi^\star$ (e.g. Sobral et al. 2009), probably in part due to cosmic variance effects, and the inherent degeneracy in LF parameter fitting. The latter is the main reason why we chose surveys with very similar fitting techniques, an attempt to mitigate the impact of different survey strategies on our model.

With this in mind, the model presented here assumes evolution *only* in $L^\star$, and the faint-end slope is held fixed at $\alpha = -1.35$ (we assess the impact of this assumption in Section 2.2.1). Given the strong luminosity evolution out to at least $z = 1.3$, and weak evolution beyond $z \sim 2$, we model the $L^\star$ evolution as $(1 + z)^Q$ over $0 < z < 1.3$ [the median redshift of the *Hubble Space Telescope* (*HST*)/Near-Infrared Camera and Multi-Object Spectrometer (NICMOS) grism survey of McCarthy et al. 1999]. At $z > 1.3$, we freeze evolution and assume that this is valid out to the limit of current Hα observations ($z = 2.23$). The best-fitting $L^\star$ evolution is

then derived as

$$L^\star(z)/\mathrm{erg \, s^{-1}} = \begin{cases} 5.1 \times 10^{41} \times (1 + z)^{3.1 \pm 0.4} & z < 1.3 \\ (6.8^{+2.7}_{-1.9}) \times 10^{42} & 1.3 < z < 2.2 \end{cases}. \qquad (2)$$

We estimate the uncertainty in Q via a bootstrap-type simulation, re-evaluating the fit 10 000 times after re-sampling each $L^\star$ in Table 1 from a Gaussian distribution of widths set by the $L^\star$ 1σ uncertainty. Note that $L^\star$ has not been corrected for intrinsic dust extinction (a canonical $A_{\mathrm{H}\alpha} = 1$ mag correction is generally applied when deriving star formation rates, although this could increase at high luminosity). The luminosities *have* been corrected for [N II] contribution, typically of the order of ∼30 per cent (e.g. Kennicutt & Kent 1983). Note that this could be a conservative correction if there is a significant contamination from active galactic nuclei (AGN). With this in mind, Hα redshift surveys should aim for a spectral resolution that can resolve Hα/[N II]. Not only does this have a significant practical benefit in that it aids redshift identification, but also the secondary science impact of a large sample of Hα/[N II] ratios and thus AGN selection would be extremely valuable.

As described above, the choice of normalization of the model is a source of uncertainty in the predicted counts. Since this paper is focused on predictions for dark energy surveys, which will target Hα emitters at $z \sim 1$, here we have taken the normalization of the model to be the average $\phi^\star$ of the surveys of Yan et al. (1999), Hopkins et al. (2000) and Shim et al. (2009). These three Hα surveys are most similar to the likely observing mode of a JDEM/Euclid-like mission (slitless spectroscopy) and operate over a similar redshift range that will be pertinent to cosmology surveys. The adopted normalization is $\phi^\star = 1.37 \times 10^{-3} \, \mathrm{Mpc^{-3}}$, and in Fig. 1 we show how this compares to a range of observed LFs spanning the full redshift range $0 < z < 2$. Down to the luminosity corresponding to the flux limit likely to be practical in cosmology surveys ($\sim 10^{-16} \, \mathrm{erg \, s^{-1} \, cm^{-2}}$), the simple model can replicate the observed space density of Hα emitters over 8 Gyr of cosmic time. At fainter limits, the uncertainty in the steepness of the faint-end slope will introduce further uncertainties that we ignore here, although we consider the effect of an evolving (steepening) faint end in Section 2.2.1.

Fig. 2 shows another comparison to data that is more relevant for predictions for dark energy surveys – i.e. the redshift-integrated counts as a function of the limiting flux over $0.75 < z < 1.90$ (i.e. accessible in the near-IR). We compare the integrated counts derived from the Yan et al. (1999), Hopkins et al. (2000) and Shim et al. (2009) LFs and the model. Note, however, that these slitless surveys cover much smaller (<1 deg^2) areas than will be achievable with dedicated survey telescopes, and so suffer significantly from cosmic variance scatter – this could account for the scatter in the observations, and highlights the problem of the choice of normalization mentioned above. The error band in our model does not include the systematic uncertainty due to choice of $\phi^\star$, but coincidentally spans the range of counts derived from the surveys shown in Fig. 2.
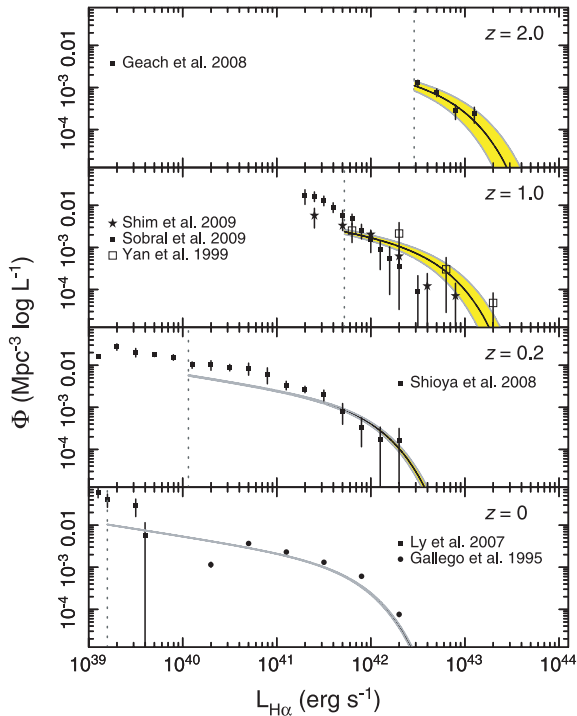
Figure 1. Evolution of the Hα LF, assuming our simple model of $L^\star \propto (1 + z)^Q$ out to $z = 1.3$ and no evolution to $z < 2.2$. The panels show the LF at $z \sim 0, 0.2, 0.9$ and 2.2, with observational data overlaid (all data have been corrected to the same fiducial cosmology used throughout this work and *not* corrected for extinction). Note that not all of the observational data shown here were used to construct the model (see Section 2.1); however, the model is a good representation of the observed LFs out to $z \sim 2$. The largest discrepancy occurs at $z \sim 1$, where there is some scatter between different surveys. However, in part, this is due to the mixture of survey strategies and cosmic variance in the small fields observed. The model LFs have been truncated at the luminosity limit corresponding to a flux of 10^{-16} erg s^{-1} cm^{-2} at each epoch (vertical dotted lines). Although there are hints that the faint-end slope is steepening out to $z \sim 1$, in the flux regime of practical interest this does not have a significant impact on our counts (also see Section 2.2.1 and Fig. 3).

For convenience, we tabulate the predicted redshift distribution dN/dz for a range of limiting fluxes, including uncertainties in Table 2. The distributions are plotted in Fig. 3. Given the large scatter in the measured space density of Hα emitters determined from different surveys (see Hopkins 2004 for a compilation), our adopted normalization should be considered the best estimate 'average'. However, when considering the feasibility of redshift surveys, the reader might want to adopt a more conservative estimate of the density normalization. If necessary, the reader can rescale the predicted counts given in Table 2. We suggest that an appropriate conservative lower limit to the counts could be taken as $\phi^\star = 1 \times 10^{-3}$ Mpc^{-3}. In Section 3 we discuss how the range of adopted normalizations affects our assessment of the feasibility of redshift surveys that aim to make cosmological measurements, and in the following section, we address further caveats that the reader should be aware of when applying this model.

2.2 Caveats

2.2.1 Evolution of the faint-end slope

Our model assumes a non-evolving faint-end slope, with $\alpha = -1.35$ determined from local measurements (Gallego et al. 1995; Shioya
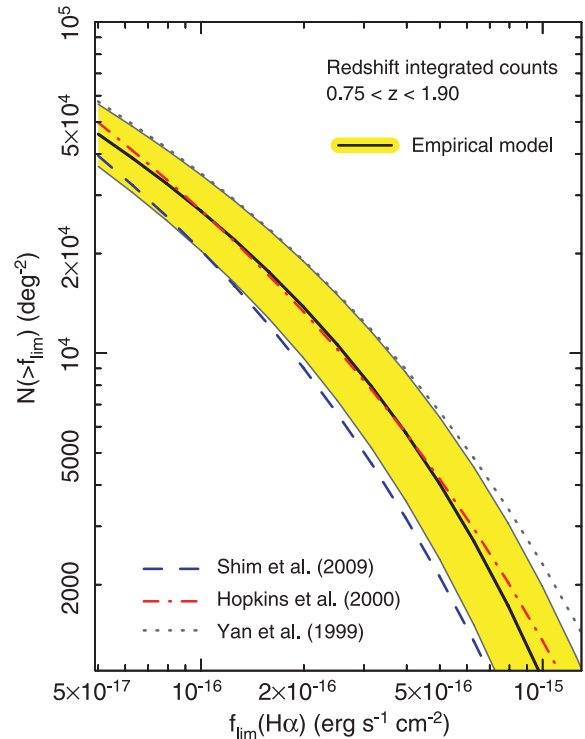
Figure 2. A comparison of the predicted number counts of Hα emitters from the simple model to observed counts integrated over the redshift range $0.75 < z < 1.90$. The shaded region indicates the 1σ uncertainty on the model counts. We compare to the observational data of the (slitless spectroscopic) surveys of McCarthy et al. (1999), Hopkins et al. (2000) and Shim et al. (2009), where the integrated counts have been calculated from the respective LFs, uncorrected for dust extinction (so the counts include incompleteness corrections specific to each survey). Note that all-sky redshift surveys are unlikely to probe below flux limits of $\sim 10^{-16}$ erg s^{-1} cm^{-2}, where uncertainties due to the poorly constrained faint-end slope become more important to the count predictions (see Section 2.2.1 for more details).

et al. 2008). Both Yan et al. (1999) and Geach et al. (2008) fix this value of α in their fits of the LF; the observations did not probe deep enough to constrain it. However, there are hints that the relative abundance of galaxies with $L < L^\star$ might increase towards early epochs (Reddy et al. 2008), with α as large as -1.6 at $z \sim 2$. What would be the ramifications of a monotonically evolving (steepening) faint-end slope out to $z \sim 2$ on our predicted counts? In Fig. 3, we compare the redshift distributions for the fixed α model and the same model with $\alpha(z)$. We ignore the correlation between $L^\star$, $\phi^\star$ and α for this analysis. At $f_{\text{lim}} > 10^{-16}$ erg s^{-1} cm^{-2}, the counts (per redshift interval) predicted from the fixed α model are never less than ~ 85 per cent of those derived from a steepening α model. At $f_{\text{lim}} > 5 \times 10^{-16}$ erg s^{-1} cm^{-2}, the counts differ by only ~ 5 per cent. This difference is smaller than the uncertainty on dN/dz, and so small enough to be ignored in this study. Needless to say, as high-z Hα studies probe deeper, past $L^\star$ and can improve the constraint on $\alpha(z)$, the simple empirical model presented here could be revised accordingly. Finally, note that Hopkins et al. (2000) derive a faint-end slope of $\alpha = -1.6$, which accounts for the turn-up in the integrated counts at $f < 10^{-16}$ erg s^{-1} cm^{-2} (Fig. 2). The empirical model is not significantly different from the Hopkins et al. (2000) counts at brighter limits, re-enforcing that our assumption of a constant (local) faint-end slope is a reasonable baseline in this regime.

Table 2. Redshift distributions dN/dz (per deg^2, calculated in bins of width $\delta z = 0.1$, centred on the value given in the first column) for a range of limiting fluxes derived from the empirical model (also see Fig. 3). For reference, we provide the range of Galactic extinctions at the observed wavelength of Hα, derived from the maps of Schlegel et al. (1998). The predicted counts include *intrinsic* extinction in the Hα emitters, but the Galactic reddening will vary as a function of sky position. Although this has a negligible (few per cent) impact on the model dN/dz, we include it here as a guide. The counts listed here are calculated for a space density normalization of $\phi^\star = 1.37 \times 10^{-3}$ Mpc^{-3} which is the 'average' space density of Hα emitters determined by several slitless surveys at $z \sim 1$ – similar to the Euclid and JDEM satellite survey concepts. The reader can rescale these counts to alternative normalizations if desired: for a more conservative estimate of the counts, we recommend a lower density normalization $\phi^\star = 1 \times 10^{-3}$ Mpc^{-3}; however as we show in Section 3, this choice does not have a significant impact on the predicted power of a galaxy redshift survey.

| | Number per $\delta z = 0.1$ interval (deg^{-2}) Limiting flux ($\times 10^{-16}$ erg s^{-1} cm^{-2}) | | | | | Reddening at $(1 + z) \times 6563$ Å $\|b\| > 20°$ (mag) | | |
Redshift	1	2	3	4	5	$A_{H\alpha}^{min}$	$\langle A_{H\alpha} \rangle$	$A_{H\alpha}^{max}$
0.10	5226^{+86}_{-85}	3838^{+67}_{-66}	3172^{+58}_{-57}	2756^{+52}_{-52}	2461^{+48}_{-47}	0.005	0.045	0.293
0.20	10160^{+367}_{-357}	7116^{+284}_{-277}	5669^{+244}_{-237}	4771^{+218}_{-211}	4142^{+199}_{-193}	0.005	0.040	0.260
0.30	14448^{+834}_{-801}	9702^{+639}_{-612}	7473^{+541}_{-517}	6107^{+478}_{-456}	5163^{+431}_{-410}	0.004	0.036	0.231
0.40	17931^{+1446}_{-1372}	11592^{+1094}_{-1033}	8657^{+915}_{-860}	6885^{+798}_{-746}	5676^{+712}_{-661}	0.004	0.032	0.207
0.50	20673^{+2160}_{-2023}	12915^{+1613}_{-1498}	9376^{+1332}_{-1227}	7270^{+1147}_{-1047}	5854^{+1010}_{-914}	0.003	0.029	0.186
0.60	22787^{+2936}_{-2714}	13803^{+2165}_{-1976}	9766^{+1766}_{-1592}	7398^{+1502}_{-1336}	5830^{+1306}_{-1147}	0.003	0.026	0.168
0.70	24386^{+3741}_{-3414}	14368^{+2727}_{-2446}	9931^{+2199}_{-1938}	7365^{+1847}_{-1600}	5689^{+1587}_{-1351}	0.003	0.023	0.152
0.80	25574^{+4553}_{-4100}	14699^{+3283}_{-2891}	9947^{+2618}_{-2254}	7236^{+2175}_{-1832}	5489^{+1849}_{-1523}	0.002	0.021	0.138
0.90	26437^{+5353}_{-4759}	14861^{+3821}_{-3305}	9868^{+3017}_{-2538}	7054^{+2482}_{-2032}	5263^{+2089}_{-1663}	0.002	0.019	0.125
1.00	27045^{+6128}_{-5381}	14905^{+4335}_{-3683}	9730^{+3392}_{-2788}	6847^{+2766}_{-2200}	5034^{+2308}_{-1776}	0.002	0.018	0.114
1.10	27456^{+6872}_{-5960}	14867^{+4823}_{-4025}	9558^{+3744}_{-3007}	6632^{+3029}_{-2341}	4811^{+2506}_{-1865}	0.002	0.016	0.104
1.20	27712^{+7579}_{-6495}	14772^{+5282}_{-4332}	9369^{+4071}_{-3196}	6420^{+3270}_{-2458}	4601^{+2687}_{-1933}	0.002	0.015	0.096
1.30	27850^{+8248}_{-6986}	14641^{+5712}_{-4606}	9173^{+4375}_{-3359}	6216^{+3493}_{-2554}	4407^{+2853}_{-1986}	0.002	0.014	0.088
1.40	24931^{+7883}_{-6612}	12514^{+5325}_{-4210}	7530^{+3978}_{-2965}	4913^{+3098}_{-2177}	3360^{+2468}_{-1636}	0.001	0.012	0.081
1.50	22178^{+7487}_{-6211}	10600^{+4919}_{-3805}	6108^{+3574}_{-2579}	3827^{+2708}_{-1822}	2517^{+2099}_{-1318}	0.001	0.011	0.074
1.60	19621^{+7071}_{-5796}	8905^{+4505}_{-3402}	4900^{+3176}_{-2210}	2939^{+2334}_{-1497}	1854^{+1755}_{-1038}	0.001	0.011	0.068
1.70	17272^{+6645}_{-5374}	7422^{+4095}_{-3011}	3888^{+2792}_{-1868}	2226^{+1985}_{-1209}	1343^{+1444}_{-801}	0.001	0.010	0.063
1.80	15136^{+6215}_{-4955}	6141^{+3693}_{-2640}	3053^{+2429}_{-1557}	1664^{+1666}_{-958}	956^{+1169}_{-604}	0.001	0.009	0.059
1.90	13209^{+5788}_{-4543}	5044^{+3307}_{-2292}	2373^{+2091}_{-1280}	1227^{+1380}_{-747}	670^{+932}_{-446}	0.001	0.008	0.054
2.00	11482^{+5368}_{-4144}	4114^{+2940}_{-1971}	1826^{+1783}_{-1039}	892^{+1128}_{-572}	461^{+731}_{-323}	0.001	0.008	0.050
2.10	9945^{+4960}_{-3761}	3332^{+2596}_{-1680}	1390^{+1505}_{-832}	640^{+911}_{-430}	312^{+564}_{-228}	0.001	0.007	0.047
2.20	8582^{+4566}_{-3397}	2681^{+2277}_{-1418}	1048^{+1258}_{-657}	453^{+726}_{-318}	208^{+429}_{-158}	0.001	0.007	0.043

2.2.2 Equivalent width cut

An important feature of emission-line surveys, and particularly narrow-band surveys, is the inclusion of an EW cut in the selection. Clearly this is an issue of sensitivity: galaxies with small EW are harder to detect and obtain reliable redshifts for. So naturally, dark energy surveys targeting emission lines are biased towards galaxies with high EWs and against weak-emission lines and/or massive galaxies. In the model presented here we have assumed a fairly low EW cut, 10 Å in the rest frame. This cut will not significantly affect the predicted counts in the flux regime of interest. For example, according to the model of Baugh et al. (2005), at a flux limit $f_{lim} = 10^{-16}$ erg s^{-1} cm^{-2}, increasing the rest-frame EW cut from 10 to 50 Å results in a drop in the number counts (integrated over $0.75 < z < 1.90$ as in Fig. 2) of ∼2 per cent; the deficit is negligible at brighter limits. In practice, redshift surveys will probably enforce an observed-frame cut of ∼100 Å.

Finally, we note that the clustering properties of bright Hα emitters will be different from those of Hα emitters with low EW, or simply continuum- (e.g. *H*-band) selected galaxies. The latter should be more highly biased tracers of the mass distribution (see Orsi et al. 2009).

2.2.3 Contamination

Emission-line surveys (aiming to detect a specific line, in this case Hα) are susceptible to contamination from galaxies with *any* strong emission lines at redshifts placing them in the spectral range of the detector. At high redshift, this can be significantly problematic – for example, nearly two-thirds of the potential $z = 2.23$ Hα emitters of Geach et al. (2008) selected with a narrow band at 2.121 μm were eliminated as low-redshift contaminants (e.g. Paα [$z = 0.13$], Paβ [$z = 0.67$], Fe II [$z = 0.3$]). Higher redshift [O III]λ5007 can also contribute to the contamination. Geach et al. (2008) used further broad-band colour and luminosity selections to select the $z = 2.23$ candidates. Although most planned dark energy surveys will employ spectroscopy, one must still consider the potential for misidentification of the Hα line in the large redshift ranges these surveys will probe.

One could use the Hα model presented here to estimate the potential level of misidentification of emission lines in spectral ranges likely to be employed in a slitless survey. For example, consider contamination from [O II] emitters at a rest-frame wavelength of 3727 Å. For a survey operating at 1–2 μm, this means contamination from galaxies in the redshift range $1.7 < z < 4.4$. If we assume that
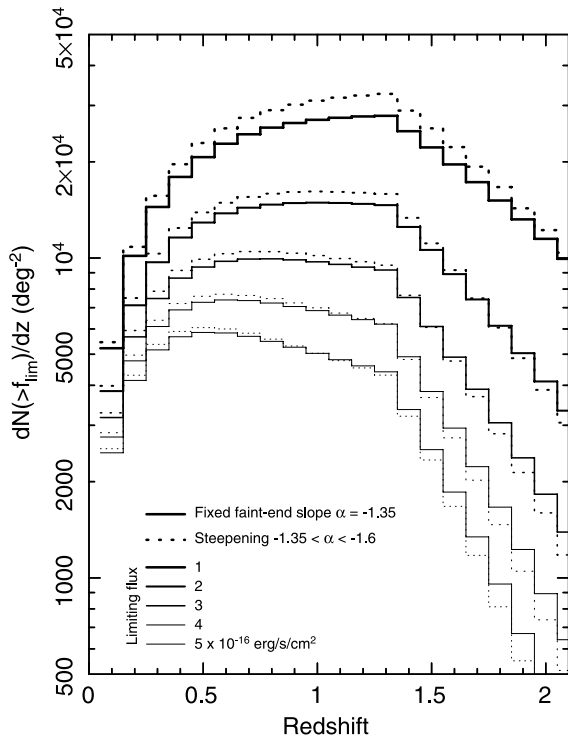
**Figure 3.** Predicted redshift distribution dN/dz of Hα emitters for limiting fluxes of 1–5 × 10^{-16} erg s^{-1} cm^{-2} (thick to thin lines). Note that the transition between $L^\star$ evolution and non-evolution at $z = 1.3$ introduces the sharp fall-off in counts towards high-z. For comparison, we also show the redshift distribution for the same $L^\star$ evolution and fixed $\phi^\star$, but allowing the faint-end slope to steepen monotonically from -1.35 at $z = 0$ to -1.6 at $z = 2$. The impact this change has on the predicted counts in the flux limits of practical interest is negligible and (as expected) more pronounced at fainter limits.

every Hα emitter is also an [O II] emitter, then we can estimate the expected number of objects in addition to the Hα emitters detected, assuming an attenuation due to the flux ratio [O II]/Hα < 1 and intrinsic extinction $A_{[O II]}$. In this example, we assume [O II]/Hα = 0.62 (measured from the 2dFGRS, at $z \sim 0.06$; Mouhcine et al. 2005). Note that this ratio has not been corrected for the relative intrinsic extinction, and so this prediction should reflect the actual number of galaxies a flux-limited survey can expect to detect.[5] As a fraction of the total number of emitters detected, the contamination from [O II] emitters ranges between 13 per cent for a limiting flux of 10^{-16} erg s^{-1} cm^{-2} and $\sim$1 per cent for 5 × 10^{-16} erg s^{-1} cm^{-2}. A plot of the decline in contamination as a function of the limiting flux is shown for reference in Fig. 4.

There are two simple ways to mitigate contamination. Perhaps the most efficient way to identify Hα is to resolve the [N II]λ6583 line (offset $\Delta\lambda = 20$ Å from Hα). Identifying this pair of lines is a useful discriminant between Hα and 'contaminant' lines, and so dark energy surveys should aim for a spectral resolution of $R > 500$ to achieve this. Another aid to redshift determination is the new generation of all-sky ground-based photometric surveys (e.g. PanSTARRS, Large Synoptic Survey Telescope). These surveys will provide op-

[5]Although strictly our model for the abundance of Hα emitters only extends to $z \sim 2$, we assume that the fixed evolution extends to $z = 4.4$. If the number of Hα emitters is actually gently declining at $z > 2$, then this contamination estimate should be considered a conservative upper limit.
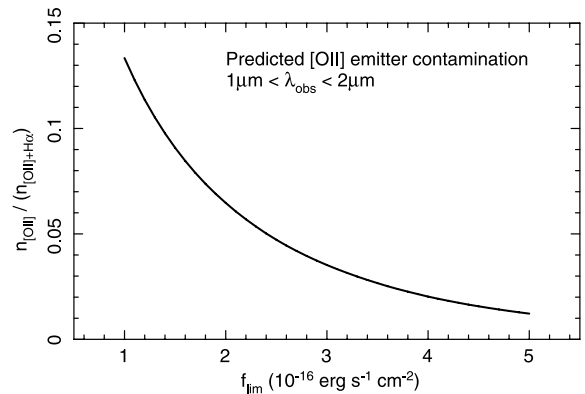
Figure 4. Prediction of contamination from [O II] emitters over the observed wavelength range of 1–2 μm. To estimate the number of [O II] emitters, we have adapted the Hα count model, extrapolating to $z = 4.4$ (the redshift of [O II] at 2 μm) making the assumption that all Hα emitters are also [O II] emitters, and these galaxies have a constant flux ratio of [O II]/Hα = 0.62 (Mouhcine et al. 2005). The contamination, expressed as a fraction of the total number of emitters detected, ranges from 1 to 13 per cent in the range of limiting fluxes of practical interest.

tical photometry of many of the sources detected in the dark energy surveys; in conjunction with the near-IR photometry, this will improve redshift estimates with a photo-z technique.

2.2.4 Extinction

The high-redshift Hα surveys described in this work have not been corrected for *intrinsic* dust extinction, although when deriving star formation rates, many authors tend to apply a canonical $A_{H\alpha} = 1$ mag unless some better estimate exists. The predicted number counts in our simple model include this intrinsic extinction, such that if the extinction properties of the Hα emitters in the surveys described in Table 1 are relatively constant over a wide range of redshift, then the predicted counts can be taken as a reliable representation of the expected yield even considering internal extinction. However, all-sky surveys (even ones that exclude the Galactic plane) will encounter a range of foreground Galactic extinction. Despite Hα being redshifted into the near-IR at $z > 0.5$, where reddening is fairly negligible, for completeness we consider here whether this could impact the predicted counts.

Taking the all-sky dust maps of Schlegel, Finkbeiner & Davis (1998),[6] we evaluate the V-band extinction for Galactic latitudes $|b| > 20°$ and extrapolate this to the observed wavelength of Hα, $\lambda = (1 + z) \times 6563$ Å out to $z = 2.2$ assuming an $R_V = 3.1$ reddening law for the Galaxy (Cardelli, Clayton & Mathis 1989; O'Donnell 1994). For reference, we summarize the average and range of reddenings for each redshift bin in Table 2. Of course, at longer wavelengths (in other words, Hα observed at higher redshifts) reddening has an ever-decreasing impact on the effective flux limit: at $z > 0.5$ the maximum $A_{H\alpha}$ is never more than 0.2 mag and the average is always <0.03 mag.

Since the regions of 'high' reddening represent a small fraction of the extragalactic sky, Galactic reddening has a minor (though redshift-dependent) impact on the predicted counts. For example, modelling the variation in $A_{H\alpha}$ over the full $|b| > 20°$ sky, at $z = 0.5$

[6]irsa.ipac.caltech.edu/applications/DUST/

there is only a 2 per cent decline in dN/dz, a smaller variation than the uncertainty of our model – we ignore its effects.
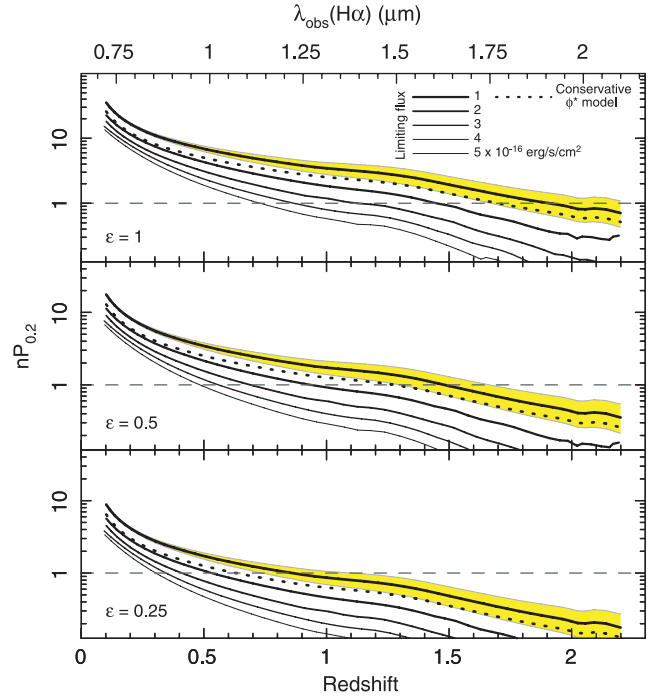
3 IMPLICATIONS FOR REDSHIFT SURVEYS

Dark energy surveys that aim to detect BAOs and measure redshift distortions in galaxy clustering could target Hα emitters in all-sky near-IR surveys, most likely utilizing grisms for slitless spectroscopy (McCarthy et al. 1999). The key issue for these surveys is the ability to measure sufficient numbers of redshifts for an accurate assessment of $w(z)$ and $f(z)$. Let us consider a hypothetical example: a slitless survey from a space platform with a wavelength coverage of 1–2 μm and a spectral resolution of $R > 500$. This range gives access to Hα at $0.5 < z < 2$, with sufficient resolution to resolve [N II]λ6583 at $f_{\rm lim} > 10^{-16}$ erg s^{-1} cm^{-2}. Aside from the slight modification to nominal limiting flux due to Galactic extinction (Section 2.2.4), there should be an additional modification to predicted counts due to some non-unity efficiency factor ϵ (the ratio of the number of successfully measured redshifts to the total number of measurable redshifts at a given flux limit). This will inevitably vary as a function of flux, EW and so on. Including some assumption for ϵ, how optimistic can we be about measurements of $w(z)$ and $f(z)$ in redshift surveys? A precise measurement of $w(z)$ or $f(z)$ requires an accurate measurement of the power spectrum, $P(k)$. The uncertainty with which $P(k)$ can be measured from a given galaxy survey depends on the number density of galaxies and the volume of the survey. If the number density is low, then the errors are dominated by shot noise. If it is high, then cosmic variance (i.e. the volume of the survey) dominates the error budget. To see this, note that the effective volume of a survey is given by Feldman, Kaiser & Peacock (1994) as

$$V_{\rm eff} = \int {\rm d}^3 r \left[\frac{\bar{n}(\boldsymbol{r})\bar{P}}{1 + \bar{n}(\boldsymbol{r})\bar{P}} \right]^2 , \qquad (3)$$

where $\bar{n}(\boldsymbol{r})$ is the comoving number density of the sample at location $\boldsymbol{r}$. For small $\bar{n}$, $V_{\rm eff} \propto \bar{n}$ and the signal is shot-noise dominated. For large $\bar{n}$, $V_{\rm eff} = V$, where V is the physical volume of the survey, which limits the signal. For a sample with a fixed total number of galaxies $N_{\rm gal} = \bar{n}V$ and for a power spectrum P, setting ${\rm d}V_{\rm eff}/{\rm d}V = 0$ requires $\bar{n}P = 1$. In this situation, we see that the effective volume reaches a maximum when $\bar{n}P = 1$. This 'sweet-spot' is often used as a design aim for fixed integration time and/or volume-limited galaxy redshift surveys, with $P_{0.2} \equiv \langle P(k)\rangle$, calculated for $k = 0.2\,h\,{\rm Mpc}^{-1}$. This scale is approximately the limit of the quasi-linear regime, and this also gives an indication of the strength of the clustering signal on the linear scales carrying the redshift-distortion information.

Future surveys will often be limited by the extragalactic sky area they can observe. For surveys using a single ground-based telescope (such as BOSS) this is of the order of $\sim 10^4$ deg^2, while for a space-based platform (such as Euclid or JDEM) or a survey using a pair of telescope in different hemispheres, this is $\sim$(2–3) × 10^4 deg^2. In this situation, the volume that can be surveyed in the interesting redshift range is limited, and the only way of gaining signal is to push to higher galaxy number densities. It is therefore important to consider values of $\bar{n}P_{0.2} > 1$.

In Fig. 5 we show the predicted $\bar{n}P_{0.2}$ as a function of redshift, for a range of (nominal) limiting fluxes (1–5) × 10^{-16} erg s^{-1} cm^{-2}. As well as the ideal case, with an efficiency factor $\epsilon = 1$ (i.e. one correctly identifies all the Hα emitters above the survey flux limit in every pointing), we show the effect on $\bar{n}P_{0.2}$ for a 50 and 25 per cent efficiency. Note that we have assumed a model for the luminosity-

Figure 5. Predictions for the effective power of a galaxy redshift survey, expressed in terms of the shot-noise parameter $\bar{n}P$ evaluated at $k = 0.2\,h\,{\rm Mpc}^{-1}$ (approximately the peak of the BAO signal). Fixed-time redshift surveys should aim for the sweet-spot of $\bar{n}P_{0.2} = 1$ to obtain maximum power from the survey. We show the predicted $\bar{n}P_{0.2}$ for limiting fluxes of 1–5 × 10^{-16} erg s^{-1} cm^{-2}, and three survey 'efficiencies' (ϵ: the actual sampling of the Hα population due to the success rate of the survey). Note the clear degeneracy between survey efficiency and flux limit. The solid lines show the predictions for our 'average' model $\phi^\star$ normalization, but we also show the predicted $\bar{n}P_{0.2}$ for a more conservative normalization, $\phi^\star = 10^{-3}$ Mpc^{-3} (for clarity only shown for $f_{\rm lim} = 10^{-16}$ erg s^{-1} cm^{-2}). The conclusion to draw from this plot is that Hα surveys should be aiming for flux limits of $\sim 10^{-16}$ erg s^{-1} cm^{-2}; beyond $z \sim 1$ the redshift yield goes into sharp decline, with severe consequences for $\bar{n}P_{0.2}$.

dependent evolution of bias for Hα emitters from Orsi et al. (2009) such that $P_{\rm gal} = P_{\rm DM}b(z, L_{\rm H\alpha})^2$. The Hα population is generated by the semi-analytic prescription GALFORM (Baugh et al. 2005). Since in the semi-analytic model one can ask which dark matter halo hosts a given galaxy, Orsi et al. estimate the galaxy bias for a given Hα luminosity by averaging over the haloes that host selected Hα emitters. The model bias for Hα emitters at $z \sim 2$ agrees well with the value derived by Geach et al. (2008) from the projected two-point correlation function. Note that we have applied the same rest-frame EW cut as applied throughout this work and interpolated the $b(z, L_{\rm H\alpha})$ as necessary. As a guide, the range of bias applied over $0 < z < 2$ for the luminosities corresponding to the limiting fluxes considered here is $0.9 \lesssim b \lesssim 1.7$.

Obviously one would always strive for maximum efficiency and depth, but this is not a practical possibility: there will always be redshift attrition resulting in $\epsilon < 1$. This inefficiency has the same impact as increasing the effective limiting flux of the survey. Losing counts has a serious impact on the survey power; even at the faintest limit likely to be practicable, 10^{-16} erg s^{-1} cm^{-2}, a 'perfect' survey struggles to achieve $\bar{n}P_{0.2} = 1$ at $z = 2$. Assuming the more likely case of $\epsilon = 0.5$, one can comfortably achieve the required $\bar{n}P_{0.2}$ out to $z = 1$, even with fairly conservative flux limits. At higher redshifts, this becomes increasingly observationally

expensive. Re-visiting the caveat of model normalization described in Section 2.1, in Fig. 5 we also show the more conservative case the reader might choose to adopt. Obviously, a shift in normalization simply translates the predicted $\bar{n}P_{0.2}$ up or down. It is worth noting that the conservative counts are within the 1σ band of uncertainty of the average model normalization at $z \geq 1$, and so our conclusions about the power of redshift surveys as a function of limiting flux and efficiency are unchanged.

One way to boost performance would be to employ Digital Micromirror Devices (DMDs) rather than traditional slitless spectroscopy. For a fixed telescope diameter and integration time, DMD-slit spectroscopy offers an improvement of sensitivity by a factor of about 3 due to the strong reduction of the sky background compared to slitless spectroscopy. This allows the detection of several spectral features in each spectrum (absorption and emission lines) and the consequent identification of all galaxy types (early-type and star-forming systems). Moreover, thanks to improved sensitivity and the lack of the 'spectral confusion' problem due to the overlap of spectra of different objects (the traditional Achille's heel of slitless spectroscopy), the redshift success rate ϵ is much higher (up to >90 per cent; see Cimatti et al. 2009).

4 COSMOLOGICAL NEAR-IR SURVEYS FROM THE GROUND

To be competitive with space platforms targeting Hα emitters at $z >$ 0.5, ground-based near-IR BAO surveys should also be aiming for limiting fluxes of 10^{-16} erg s^{-1} cm^{-2}, but there are extra observational challenges – not least the deleterious effect of the atmosphere in the near-IR. Approximately 30 per cent of the 1–2 μm window have an atmospheric transmission of <80 per cent, mainly affecting Hα in the redshift ranges $1 < z < 1.3$ and $1.7 < z < 2.1$. In addition, near-IR observations from the ground must also contend with forest of OH airglow: even at $R \sim 2000$ less than half of the near-IR spectral range is free from OH line emission, although new OH suppression technologies could partly mitigate this effect.

On the basis of areal coverage, ground-based near-IR BAO survey will never be competitive with a Euclid/JDEM-like mission. Modern wide-field near-IR spectrographs deploy fibres on individual targets, and this presents a significant disadvantage compared to the slitless approach of the space missions: one must select targets prior to observation (in some sense, the problem is reversed in the slitless case). Typically this will require the target fields to be complemented by multicolour broad-band photometry, deep enough to provide an estimate of redshift. Note that the consequence for misidentifying targets is a strong hit to the efficiency parameter ϵ.

In the event of a dedicated space-based near-IR dark energy survey going ahead, one could argue that a more efficient use of ground based multi-object spectrographs in the near-IR would be to complement the wider cosmological surveys by providing more detailed follow-up observations of a sub-sample of line emitters. This has the advantage of side-stepping the issue of target selection, since the sample would already be 'sanitized' by the cosmology survey. Such a symbiosis between space and ground would be an efficient use of resources since (i) the ground facilities would target known line emitters and therefore rapidly build up a large sample of spectroscopic observations for high-redshift galaxies in more detail than can be achieved from the space platforms and (ii) the complementary observations could help to better characterize contamination from other line emitters (as discussed in Section 2.2.3), thus feeding back information to the cosmological survey. Combining surveys in this way could serve to satisfy two groups of researchers: those interested in the astrophysics of galaxies at high redshift and those concerned with cosmological measurements.

5 SUMMARY AND FINAL REMARKS

We have presented a simple prescription for the prediction of the abundance of Hα emitters over $0 < z < 2$, based on empirical data. The model is simplistic, due to limited available data; it assumes a fixed space density, fixed faint-end slope and only $L^\star$ evolution out to $z = 1.3$. There is no luminosity evolution to higher redshifts, consistent with current Hα observations at this redshift. Despite its simplicity, the model adequately mimics the observed LFs of a range of Hα surveys (including a mixture of spectroscopic, grism and narrow-band strategies). Using the LF model as a basis, we predict the redshift distribution of Hα emitters corresponding to a spectral coverage that extends to 2 μm.

Our results have particular relevance to dark energy experiments attempting to measure cosmological information from the power spectrum of galaxies detected in all-sky Hα surveys in the near-IR. We use the parameter $\bar{n}P_{0.2}$ as a measure of the effectiveness of a redshift survey and make predictions for this value for a range of redshifts, limiting fluxes and success rates (i.e. efficiencies). To achieve $\bar{n}P_{0.2} = 1$ out to $z = 2$, emission-line surveys should be aiming for limiting fluxes of $\sim 10^{-16}$ erg s^{-1} cm^{-2}. However, this estimate is reliant on a high success rate of the sampling of the Hα population: redshift surveys need to aim for high efficiencies, since any decline in redshift yield (i.e. failing to obtain redshifts for detections) has the same effect on $\bar{n}P_{0.2}$ as increasing the flux limit (illustrated in Fig. 5 of this work). Assuming a more likely situation of 50 per cent efficiency, a realistic target for proposed surveys is $\bar{n}P_{0.2} = 1$ at $z = 1.5$. At higher redshifts, the sharply declining number counts have a severe effect on one's ability to measure $w(z)$ at the desired precision.

REFERENCES

Albrecht A. et al., 2006, Report of the Dark Energy Task Force, preprint (astro-ph/0609591)
Albrecht A. et al., 2009, Findings of the Joint Dark Energy Mission Figure of Merit Science Working Group, preprint (arXiv:0901.0721)
Baugh C. M., Lacey C. G., Frenk C. S., Granato G. L., Silva L., Bressan A., Benson A. J., Cole S., 2005, MNRAS, 356, 1191
Blake C., Glazebrook K., 2003, ApJ, 594, 665
Bond J. R., Efstathiou G., 1984, ApJ, 285, L45
Bond J. R., Efstathiou G., 1987, MNRAS, 226, 655
Bower R. G., Benson A. J., Malbon R., Helly J. C., Frenk C. S., Baugh C. M., Cole S., Lacey C. G., 2006, MNRAS, 370, 645
Cardelli J. A., Clayton G. C., Mathis J. S., 1989, ApJ, 345, 245
Cimatti A. et al., 2009, Exp. Astron., 23, 39
Cole S. et al., 2005, MNRAS, 362, 505
Colless M. et al., 2003, preprint (astro-ph/0306581)
Copeland E. J., Mizuno S., Shaeri M., 2009, Phys. Rev. D, 79, 10
Dvali G. R., Gabadadze G., Porrati M., 2000, Phys. Lett. B, 485, 208

Eisenstein D. J. et al., 2005, ApJ, 633, 560
Eisenstein D. J., Seo H.-J., White M., 2007, ApJ, 664, 660
Feldman H. A., Kaiser N., Peacock J. A., 1994, ApJ, 426, 23
Gallego J., Zamorano J., Aragon-Salamanca A., Rego M., 1995, ApJ, 455, L1
Gaztanaga E., Cabre A., Hui L., 2009, MNRAS, 399, 1663
Geach J. E., Smail I., Best P. N., Kurk J., Casali M., Ivison R. J., Coppin K., 2008, MNRAS, 388, 1473
Glazebrook K. et al., 2007, in Metcalfe N., Shanks T., eds, ASP Conf. Ser. Vol. 379, Cosmic Frontiers. Astron. Soc. Pac., San Francisco, p. 72
Goldberg D. M., Strauss M. A., 1998, ApJ, 495, 29
Guzzo L. et al., 2008, Nat, 451, 541
Hicken M. et al., 2009, ApJ, 700, 1097
Hill G. J. et al., 2008, in Kodama T., Yamada T., Aoki K., eds, ASP Conf. Ser. Vol. 399, Panoramic Views of Galaxy Formation and Evolution. Astron. Soc. Pac., San Francisco, p. 115
Holtzman J. A., 1989, ApJS, 71, 1
Hopkins A. M., 2004, ApJ, 615, 209
Hopkins A. M., Connolly A. J., Szalay A. S., 2000, AJ, 120, 2843
Hu W., Haiman Z., 2003, Phys. Rev. D, 68, 3004
Huetsi G., 2006, A&A, 449, 891
Kaiser N., 1987, MNRAS, 227, 1
Kazin E. A. et al., 2009, preprint (arXiv:0908.2598)
Kennicutt R. C., Jr, Kent S. M., 1983, AJ, 88, 1094
Lilly S. J., Tresse L., Hammer F., Crampton D., Le Fevre O., 1995, ApJ, 455, 108
Ly C. et al., 2007, ApJ, 657, 738
McCarthy P. et al., 1999, ApJ, 520, 548
Meiksin A., White M., Peacock J. A., 1999, MNRAS, 304, 851
Moorwood A. F. M., van der Werf P. P., Cuby J. G., Oliva E., 2000, A&A, 326, 9
Mouhcine M., Lewis I., Jones B., Lamareille F., Maddox S. J., Contini T., 2005, MNRAS, 362, 1143
O'Donnell J. E., 1994, ApJ, 422, 1580

Orsi A., Baugh C. M., Lacey C. G., Cimatti A., Wang Y., Zamorani G., 2009, preprint (arXiv:0911.0669)
Peebles P. J., Ratra B., 2003, Rev. Modern Phys., 75, 559
Peebles P. J., Yu J. T., 1970, ApJ, 162, 815
Percival W. J. et al., 2001, MNRAS, 327, 1297
Percival W. J., Cole S., Eisenstein D., Nichol R., Peacock J. A., Pope A., Szalay A., 2007, MNRAS, 381, 1053
Percival W. J. et al., 2009, MNRAS, submitted, preprint (arXiv:0907.1660)
Perlmutter S. et al., 1999, ApJ, 517, 565
Reddy N. A., Steidel C. C., Pettini M., Adelberger K. L., Shapley A. E., Erb D. K., Dickinson M., 2008, ApJS, 175, 48
Riess A. G. et al., 1998, AJ, 116, 1009
Schlegel D. J., Finkbeiner D. P., Davis M., 1998, ApJ, 500, 525
Schlegel D., White M., Eisenstein D., 2009, Astro2010: The Astronomy and Astrophysics Decadal Survey, Science White Papers, no. 314
Seo H.-J., Eisenstein D. J., 2003, ApJ, 498, 720
Seo H.-J., Eisenstein D. J., 2005, ApJ, 633, 575
Shim H., Colbert J., Teplitz H., Henry A., Malkan M., McCarthy P., Yan L., 2009, ApJ, 696, 785
Shioya Y. et al., 2008, ApJS, 175, 128
Silk J., 1968, ApJ, 151, 459
Sobral D. et al., 2009, MNRAS, 398, 75
Springel V. et al., 2005, Nat, 435, 629
Sunyaev R. A., Zel'dovich Ya. B., 1970, Ap&SS, 7, 3
Wang Y., 2006, ApJ, 647, 1
Wang Y., 2008, J. Cosmol. Astropart. Phys., 5, 21
White M., 2005, Astropart. Phys., 24, 334
Yan L., McCarthy P. J., Freudling W., Teplitz H. I., Malumuth E. M., Weymann R. J., Malkan M. A., 1999, ApJ, 519, L47
York D. G. et al., 2000, AJ, 120, 1579

This paper has been typeset from a TEX/LATEX file prepared by the author.